Fabrication and characterization of extracellular matrix scaffolds obtained from adipose-derived stem cells

Riis, Simone; Hansen, Anne Cathrine; Johansen, Lonnie; Lund, Kaya; Pedersen, Cecilie; Pitsa, Aikaterini; Hyldig, Kathrine; Zachar, Vladimir; Fink, Trine; Pennisi, Cristian Pablo

Published in:
Methods

DOI (link to publication from Publisher):
10.1016/j.ymeth.2019.07.004

Publication date:
2020

Document Version
Accepted author manuscript, peer reviewed version

Accepted Manuscript

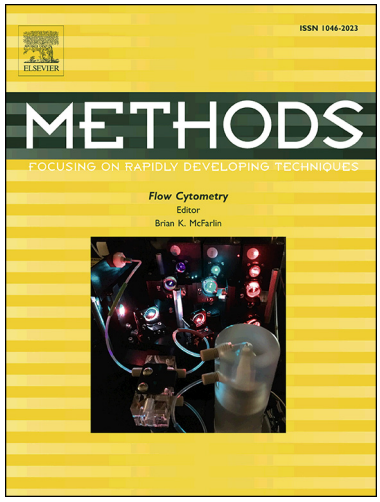

Fabrication and characterization of extracellular matrix scaffolds obtained from adipose-derived stem cells

Simone Riis, Anne Cathrine Hansen, Lonnie Johansen, Kaya Lund, Cecilie Pedersen, Aikaterini Pitsa, Kathrine Hyldig, Vladimir Zachar, Trine Fink, Cristian Pablo Pennisi

PII: S1046-2023(18)30431-6
DOI: https://doi.org/10.1016/j.ymeth.2019.07.004
Reference: YMETH 4756

To appear in: *Methods*

Received Date: 8 March 2019
Revised Date: 17 April 2019
Accepted Date: 6 July 2019

Please cite this article as: S. Riis, A.C. Hansen, L. Johansen, K. Lund, C. Pedersen, A. Pitsa, K. Hyldig, V. Zachar, T. Fink, C.P. Pennisi, Fabrication and characterization of extracellular matrix scaffolds obtained from adipose-derived stem cells, *Methods* (2019), doi: https://doi.org/10.1016/j.ymeth.2019.07.004

Fabrication and characterization of extracellular matrix scaffolds obtained from adipose-derived stem cells

Simone Riis, Anne Cathrine Hansen, Lonnie Johansen, Kaya Lund, Cecilie Pedersen, Aikaterini Pitsa, Kathrine Hyldig, Vladimir Zachar, Trine Fink, and Cristian Pablo Pennisi*

Laboratory for Stem Cell Research, Department of Health Science and Technology, Aalborg University, Aalborg, Denmark

***Correspondence:**

Cristian Pablo Pennisi, Laboratory for Stem Cell Research, Department for Health Science and Technology, Aalborg University, Fredrik Bajers Vej 3B, 9220 Aalborg Ø, Denmark. Telephone: +45 99402419

e-mail: cpennisi@hst.aau.dk

Keywords: extracellular matrix; decellularization; adipose-derived stem cells; wound healing; scaffold

Abstract

Chronic non-healing wounds are detrimental for the quality of life of the affected individuals and represent a major burden for the health care systems. Adipose-derived stem cells (ASCs) are being investigated for the development of novel treatments of chronic wounds, as they have shown several positive effects on wound healing. While these effects appear to be mediated by the release of soluble factors, it is has also become apparent that the extracellular matrix (ECM) deposited by ASCs is essential in several phases of the wound healing process. In this work, we describe an approach to produce ECM scaffolds derived from ASCs in culture. Upon growth of ASCs into an overconfluent cell layer, a detergent-based cell extraction approach is applied to remove the cellular components. The extraction is followed by an enzymatic treatment to remove the residual DNA. The resultant cell-derived scaffolds are depleted of cellular components, display low DNA remnant, and retain the native fibrillar organization of the ECM. Analysis of the molecular composition of the ECM scaffolds revealed that they are composed of collagens type I and III, and fibronectin. The decellularized scaffolds represent a substrate that supports adhesion and proliferation of primary human fibroblasts and dermal microvascular endothelial cells, indicating their potential as platforms for wound healing studies.

1. Introduction

Normal wound healing progresses through a series of highly regulated partially overlapping phases involving a complex interplay between the different cells residing in or migrating into the wound bed [1]. A multitude of conditions, including diabetes, trauma or vascular insufficiency, may perturb the healing process in such a manner that the wound healing halts, and the wound becomes chronic [2]. Chronic wounds are defined as wounds that have failed to heal within 3 months and, as such, they impose a major strain on patients, whose quality of life becomes invariably deteriorated. Importantly, chronic wounds represent a major burden to the health care systems, since the associated costs represent a relatively big proportion of the health budget. In the EU, for example, it is estimated that the treatment of chronic wounds drains approximately 2 % of the financial resources [3,4].

The current treatment approaches, which are largely based on dressings to maintain the humidity of the wound and to protect against further trauma, are often inefficient [1]. In the quest to develop new and more efficient treatments, the use of adipose-derived stem cells (ASCs) seems to offer a new promise. ASCs have namely been shown to exert a number of properties that are critical for would healing, such as the capability to reduce inflammation, promote angiogenesis and fibroblast proliferation and migration [5,6]. Not surprisingly, the augmentation of healing has been demonstrated *in vitro*, and was initially attributed to the soluble factors secreted from ASCs [7,8]. However, as ASCs produce both structural elements as well as factors involved in extracellular matrix (ECM) maturation [9], and ECM integrity and composition play a role in wound healing, it is plausible that the wound healing effects of ASCs are, at least in part, mediated through effects on the ECM [10]. Although there is an increasing body of evidence from preclinical and early-stage clinical trials, which strongly indicate that application of ASCs to chronic wounds accelerate the wound closure [11], little is known about the specific contribution of the ECM in this process. Interestingly, cell-free ECM scaffolds obtained from cultured bone marrow-derived mesenchymal stem cells (BM-MSCs), which share similarities to ASCs in terms of wound healing properties [12], have been shown to promote cutaneous wound healing in an animal model [13]. While the improved healing appears to be mediated by enhanced re-epithelialization and angiogenesis, the detailed molecular picture of the processes remains elusive, and it would be of interest to obtain a deeper understanding of the role played by the ECM. To that end, the establishment of a wound healing model that would allow exploration of decellularized ASC ECM would be highly desirable.

Decellularized matrices derived from cell cultures have gained increasing attention in biomedical research over the past years [14]. They have been mainly employed as *in vitro* models in studies aimed at investigating the role of ECM components in the control of cell fate [15–17]. In general, following a period of culture of the cells on an appropriate substrate, the cellular components are

removed by physical, chemical and/or enzymatic treatments. The resulting matrix, often referred as a cell-derived ECM scaffold, consists of a complex assembly of fibrillar proteins, associated macromolecules and growth factors resembling the natural ECM microenvironment [18–20]. The major parameters that influence the properties and composition of the ECM scaffold are the cell type used, the culture conditions, and the decellularization approach [21]. Various protocols for the production of cell-derived ECM scaffolds, based on fibroblasts of BM-MSCs cultures, are available in the literature [20,22,23]. However, given the different origin and location of these cells, their ECM display compositional and structural differences to that produced by ASCs [24,25]. Furthermore, none of the previously reported protocols fits accurately the requirements of our intended application in terms of preservation of the ECM structural integrity, removal of cellular remnant, and suitability for downstream wound healing relevant assays.

In this paper, we present an approach for the production and decellularization of ECM from ASCs, which constitute a platform to study the particular properties of the ECM in the absence of the confounding effects of ASCs and their continuous production of soluble factors. The focus has been to devise an approach that produces an ECM scaffold suitable for the development of *in vitro* wound healing models.

2. Materials and methods

2.1 Culture of ASCs

Human ASCs cultures were initiated from adipose tissue obtained from three healthy donors undergoing elective liposuction. The cell isolation protocol has been described in detail elsewhere [26]. The protocol was approved by the regional Committee on Biomedical Research Ethics of Northern Jutland, Denmark (project no. VN 2005/54). These ASC cultures have been thoroughly characterized by our group in terms of their stem cell properties, which include multilineage differentiation capacity, clonogenicity, and immunophenotype [27–33]. Cells were cultured using growth medium consisting of α-Minimum Essential Medium (MEM-alpha with GlutaMAX, no nucleosides, Gibco, ThermoFisher Scientific) supplemented with 10 % fetal calf serum (FCS), 100 IU/ml penicillin, and 0.1 mg/ml streptomycin (all from ThermoFisher Scientific). The cells were maintained in polystyrene flasks (Greiner Bio-one) in a standard humidified incubator at 37 °C, 20% O2 and 5 % CO2, with medium changes twice a week. Cells were passaged using TrypLE select (Gibco, ThermoFisher Scientific) when achieving 80% confluence. All experiments were conducted using cells between passage 3 and 5.

2.2 Induction of cells for ECM production

ASCs were seeded at a density of 6,000 cells/cm^2 in 24-well tissue culture plates (Greiner Bio-one). After 24 h, to induce the production of ECM, the culture medium was replaced by growth medium supplemented with 0.2 mM ascorbic acid (AA), (L-ascorbic acid 2-phosphate sesquimagnesium salt hydrate, Sigma-Aldrich). Cells were induced for 10 days, with medium changes every other day. Cells in growth medium without AA were used as control. Prior to cell seeding, to avoid spontaneous detachment of the cell-ECM sheets during the induction period, the culture surfaces were pre-coated with poly-L-lysine (PLL). In brief, a PLL solution 0.01 % w/v (A-005-C, Millipore) was added to the culture wells and incubated for 5 min at room temperature. Wells were rinsed with sterile deionized water, left to dry for 2 h, and stored at 4 ^{o}C until cell seeding.

2.3 Preparation of decellularized ECM scaffolds

An extraction buffer (EB) consisting of 1% Triton X-100 (TX-100) and 20 mM ammonium hydroxide (NH_4OH) in phosphate buffered saline (PBS) was preheated to 37 °C. Cells were rinsed with PBS and decellularization was carried out by incubating the cells with the EB for 5 min at 37^{o}C. PBS was added to the wells to dilute the EB (1:1) and the mixture was carefully aspirated. A subsequent wash with PBS was carried out on a shaking platform (The Belly Dancer, Stovall Life Science) at low speed (10 rpm) for 1 h at room temperature. Next, the wells were treated with a deoxyribonuclease (DNase) solution for 30 min at 37^{o}C. DNase solution consisted of DNAse I from bovine pancreas (D4263, Sigma-Aldrich) in PBS containing 5 mM $MgCl_2$ and 130 μM $CaCl_2$. Three different DNase concentrations were assessed (10, 20, and 100 IU/mL). After enzymatic treatment, the wells were rinsed twice with

PBS and left overnight in PBS on the shaking platform at low speed (10 rpm) at 4 °C. The ECM scaffolds were subsequently stored at 4 °C until further experiments.

2.4 Assessment of decellularization

For a qualitative evaluation of the decellularization efficiency, ECM scaffolds were stained with a nuclear stain before and after decellularization. The samples were stained for 10 min at room temperature using Hoechst 33342 (Sigma-Aldrich) diluted to 10 µg/ml in PBS. After incubation, the samples were rinsed twice with PBS and visualized under a fluorescence microscope (AxioObserver, Carl Zeiss). Images were captured using digital camera (C11440 ORCA Hamamatsu) and ZEN 2012 software (Carl Zeiss). For a quantitative analysis, the amount of dsDNA before and after DNAse treatment was measured using a Quant-iT™ PicoGreen dsDNA assay kit (Invitrogen, ThermoFisher Scientific). The decellularized matrices were scraped off the wells and transferred to ultracentrifuge tubes containing 0.1% TX-100 in 1× Tris/EDTA buffer (TE buffer, included in the kit). The samples were subsequently subjected to three freezing-thawing cycles (from -20°C to 37°C). Thawing was carried out in an ultrasonic bath (1510, Branson). The PicoGreen reagent was added to the samples (1:1) and the mixture was incubated for 10 min, at room temperature and in the dark. Aliquots of the mixture were transferred in duplicates to 96-well microtiter plates and the fluorescence was measured using a multimode plate reader (EnSpire, PerkinElmer) with excitation and emission at 485 nm and 535, respectively.

2.5 Quantification of ECM production

2.5.1 Assessment of collagen by the Sirius Red/Fast Green assay

A Sirius Red/Fast Green staining (Chondrex Inc.) was conducted to evaluate the amount of collagen and non-collagenous proteins in the ECM scaffolds. Staining was performed according to manufacturer's protocol, including a fixation step. Images were obtained using an inverted microscope (Olympus) using a digital camera (PixeLINK) and the PixeLINK capture OEM software. Destaining of samples was done according to manufacturer's protocol and the optical densities (OD) were read at wavelengths 540 nm and 605 nm using the Enspire reader. Results were analyzed using EnSpire Manager software (PerkinElmer) and Microsoft Excel 2016. Following the manufacturer's protocol, the amount of collagen was obtained by subtracting the contribution of the Fast Green at 540 nm (which is 29.1% of the OD 605 nm value) to the OD 540 value, and dividing the resulting number by 0.0378, which is the color equivalence (OD value/µg protein) for collagenous protein.

2.5.2 Assessment of total ECM protein by the BCA assay

A radioimmunoprecipitation assay (RIPA) buffer comprising 20 mM Tris HCl (pH=7.4), 150 mM NaCl, 1 mM EDTA, 0.1% TX-100, 0.1 % SDS, and 0.5% sodium deoxycholate was prepared. Decellularized ECM scaffolds were scraped off from the wells and transferred to microcentrifuge tubes containing RIPA buffer. The tubes were sonicated at an output of 40 W for 5 min (UP200S, Hielscher

GmbH). After sonication, the tubes were centrifuged at 10,000 rpm and the pellets were discarded. The total protein concentration in the supernatant was determined using Pierce BCA Protein Assay Kit (ThermoFisher). The working BCA reagent was prepared by mixing components A and B in a 50:1 ratio. Standards were prepared with a working rage of 20 - 2000 μg/ml. In a 96-well microtiter plate, the samples and standards were mixed with the working reagent in 1:10 ratio and incubated for 30 min at 37^{o}C. The absorbance was measured at 562 nm in the Enspire reader.

2.6 Immunostaining of ECM proteins

Composition of the ECM was assessed using indirect immunofluorescence staining and wide-field fluorescence microscopy. Decellularized ECM samples were fixed in 4 % formaldehyde and subsequently incubated with 1% bovine serum albumin (BSA) in PBS (PBS-BSA) for 30 min to prevent non-specific IgG adsorption. After blocking, the samples were incubated either with a mouse monoclonal antibody anti-type I collagen (C-2429, Sigma-Aldrich), or with a goat anti-type III collagen (1330-01, SouthernBiotech), or with an anti-fibronectin antibody produced in rabbit (F3648, Sigma-Aldrich). All primary antibodies were diluted 1:200 in PBS-BSA. Incubation with both anti-collagen antibodies took place overnight at 4 ^{o}C, while incubation with anti-fibronectin antibody lasted for 1 h at 37 ^{o}C. After two PBS washings, the samples were incubated in a staining solution containing an anti-mouse Alexa Fluor 488 antibody produced in donkey (A21202, Invitrogen, ThermoFisher Scientific), an anti-goat Alexa Fluor 488 antibody produced in rabbit (A11078, Invitrogen, ThermoFisher Scientific), or an anti-rabbit Alexa Fluor 555 antibody produced in goat (A-21428, Invitrogen, ThermoFisher Scientific), respectively. Incubation with the secondary antibodies was carried out using 1:500 dilutions in PBS-BSA, for 1 h at room temperature. Fluorescence images were obtained using an inverted microscope (AxioObserver.Z1, Carl Zeiss) equipped with a digital camera (ORCA C11440 Hammatsu) and the ZEN 2012 software package (Carl Zeiss).

2.7 Assessment of transcriptional activity of ECM related genes

2.7.1 Cell lysis, RNA isolation and cDNA synthesis

To investigate the transcriptional activity of type I and III collagens, matrix metalloproteinase-1 (MMP-1), and fibronectin, the ASCs were seeded as described in 2.2. After 24, 48, and 72 h, the cells were lysed and total RNA was extracted using the Aurum Total RNA purification kit (Bio-Rad), following the manufacturer instructions. The total RNA concentration and purity were measured in a NanoDrop spectrophotometer (ND-1000 spectrophotometer, Fisher Scientific). The total RNA concentration ranged from 5-10 ng/μL. The cDNA was synthesized from the isolated RNA using the iScript cDNA synthesis kit (Bio-Rad), following the manufacturer instructions. Synthesis was performed in a thermal cycler (GeneAmp 2400, Perkin Elmer), incubating the samples for 5 min at 25 ˚C, 30 min at 42 ˚C, and 5 min at 85 ˚C.

2.7.2 qPCR

All primers (Table I) were designed using the open-source software Primer3 and produced by the LGC Biosearch Technologies (Risskov, Denmark). RT-qPCR was performed in a final volume of 25 µL containing the cDNA templates, iTaq Universal SYBR Green Supermix (Bio-Rad), and the corresponding reverse and forward primers (10 pmol). The amplification reactions were performed in a CFX Connect real-time PCR machine (Bio-Rad). The thermal cycling consisted of an initial denaturation step at 95 °C for 5 min. The amplification was performed for 40 cycles of denaturation at 95 °C for 10 sec followed by primer annealing for 30 sec. Product specificity was verified by melting curve analysis. The relative expression level for each gene was calculated based on a standard curve, which was derived from a cDNA pool obtained from all samples. In each assay, a negative control without cDNA was included. The normalization was based on the expression of the reference gene PPIA [34]. Gene expression analysis was performed using the Gene Study function in the CFX Manager software (v 3.1, Bio-Rad). Results were expressed as relative normalized expression levels with respect to the reference gene. Gene regulation analysis was performed using the gene expression levels at 24 h as a reference.

2.8 Culture of cells on ECM scaffolds

The ability of the decellularized matrices to support adhesion and growth of cells was assessed by phase contrast microscopy and a cell proliferation assay. The ECM scaffolds were sterilized in a UV crosslinking device (Stratalinker 1800, Stratagene), exposing the samples to a 254-nm light source for 5 min. Human dermal microvascular endothelial cells (HDMEC, PromoCell, Heidelberg, Germany) were seeded at a density of 10,000 cells/cm^2 using endothelial cell growth medium (MV2; PromoCell). Primary human fibroblasts (ATCC no. CRL 2429) were seeded at a density of 7,500 cells/cm^2 using culture medium consisting of high-glucose Dulbecco's Modified Eagle's medium (DMEM, Invitrogen, ThermoFisher Scientific) supplemented with 10% fetal calf serum, 100 IU/ml penicillin, and 0.1 mg/ml streptomycin. Cytotoxicity/viability was assessed by using the combination of calcein-AM (C1430, Invitrogen, ThermoFisher Scientific) and propidium iodide (PI) (4170, SigmaAldrich), which stain viable and dead cells, respectively. After 24 h in culture, cells were incubated with a staining solution containing 0.5 µg/mL calcein-AM and 10 µg/mL PI, at 37^{o}C for 1 h. Following a wash with PBS, fluorescence images were obtained using the same equipment used for the acquisition of images of immunolabelled ECM (section 2.6). Cell proliferation was quantitatively measured using the alamarBlue assay (Invitrogen, ThermoFisher Scientific). After 24, 48, or 72 h in culture, the alamarBlue reagent was added to the culture medium in a volume equal to 10% of the total culture volume. Cultures were then incubated for 2 h at 37 °C before aliquots of 100 µl were transferred to a 96-well microtiter plate. Fluorescence intensity was recorded at 590 nm with excitation at 544 nm in the Enspire reader. Growth rates were expressed as doubling times, which were estimated by fitting the data with an

exponential growth curve, as previously reported [35]. For the proliferation assay, bovine collagen I-based cell carriers (CCC for 24-well plates, Viscofan BioEngineering) were used as controls.

2.9 Statistics

Statistical analysis was performed using GraphPad Prism 7 (GraphPad Software, La Jolla, CA). The PicoGreen data were analyzed using a one-way ANOVA with a Tukey's multiple comparisons test, assuming homogeneity of variances. The amount of collagen obtained from the Sirius Red/Fast Green staining was compared using an unpaired t-test, assuming equal standard deviations. Normality of the datasets was confirmed using the Kolmogorov-Smirnov test. The regression analysis of cell proliferation data was performed using an unconstrained least-squares fit, in which a sum-of-squares F test was used to compare the estimated doubling times. Unless otherwise specified, statistical significance was assigned to differences with $P < 0.05$

3. Results and discussion

3.1 Assessment of culture conditions to prevent cell detachment

In contrast to ASCs in the control wells (Figure 1, control) or in the PLL-coated wells (Figure 1, PLL), supplementation of the culture medium with AA over the 10-day period supported the growth of an overconfluent cell layer (Figure 1, AA, PLL). The significant effect of AA on promoting cell growth and ECM synthesis has been described in the literature for ASCs and various other types of adherent cells, including BM-MSCs and fibroblasts [36–38]. AA has a well-documented role as coenzyme in the process of collagen synthesis, supporting the maintenance of connective tissue and playing a key role in wound healing processes [39]. The deposited matrices, however, had a considerable tendency to detach from culture surface in the uncoated wells after 5 to 6 days (Figure 1, AA). This behavior has been also observed in overconfluent BM-MSCs cultures supplemented with AA, which form a multilayer structure that detaches from the dish and ultimately collapses into a floating aggregate [40]. A similar behavior has been reported in cultures of AA-stimulated fibroblasts, as a consequence of the cells' pulling force on the deposited matrix [23]. Studies have shown that coating the culture surfaces with 0.1% gelatin hinders the detachment of the cells and its ECM [16,23]. However, since biological coatings have an impact on the expression of ECM molecules [41], we explored the feasibility of using a non-specific coating (PLL) to promote cell adherence to the dish. We found that the PLL provided a stable anchoring support to the cell layers, preventing the detachment of the cells and its deposited ECM not only during the 10-day culture period but also during the subsequent decellularization procedures.

3.2 Decellularization and confirmation of cell removal

Among the various methods for preparation of ECM scaffolds derived from cell cultures, surfactant-based methods are preferred over physical procedures, such as high-hydrostatic pressure or freeze-thaw, since they provide a more efficient removal of the different cellular components [19,20]. Here, an EB based on the nonionic detergent TX-100 combined with ammonium hydroxide was employed as the first step to decellularize the ASC cultures. As compared to other decellularization agents, this EB provides a milder decellularization, which solubilizes the cell membranes by breaking up lipid-protein and lipid-lipid associations [42]. Furthermore, it is important to minimize the presence of residual DNA in the decellularized scaffold [43], as DNA fragments have shown to inhibit the growth of cells [44], and also represent a risk for triggering immune responses *in vivo* [45]. Paradoxically, this step is often considered optional and thus not included in the decellularization of ECM-producing cells [16,22,23]. Here, we included a DNase treatment as the second step in the decellularization process. To determine which is the proper concentration required for an optimal removal of residual DNA, we assessed the efficiency of DNase at three different concentrations, keeping constant the incubation time and the temperature. While positive Hoechst staining was observed in the wells without DNase treatment, there was a considerably reduced fluorescence intensity captured from the wells treated with the enzyme

solution (Figure 2a). The results of the PicoGreen assay showed that upon DNAse treatment there was a significant reduction of residual DNA in the decellularized scaffolds (Figure 2c). The ECM scaffolds exposed to the highest DNAse concentration displayed the lowest dsDNA amount (4.8 ± 0.3 ng dsDNA/well), which implies the removal of more than 99% of the DNA originally present in the cell culture. To normalize the amount of residual DNA, previous studies have utilized the total amount of protein, which represents a fraction of the total mass of a biological scaffold [46]. Taking in consideration that the total amount of protein in the decellularized scaffolds was 105.3 ± 7.0 μg/well (n = 10), as determined by the BCA assay, the concentration of dsDNA in the wells treated with 100 U/mg DNAse was approximately 46 ng per mg of protein. It is therefore reasonable to assume that the concentration of residual dsDNA in this group is below the threshold of 50 ng of dsDNA per mg of scaffold, which is considered to reflect an efficiently decellularized biological material [43]. Phase contrast microscopy revealed that the wells were efficiently decellularized after incubation with the EB and DNase, leaving only the fibrillar extracellular components in the scaffold (Figure 2b).

3.3 Assessment of ECM composition

Imaging the decellularized scaffolds after Sirius Red/Fast Green staining allowed visualization of the collagen fibers (Figure 3a). The fibers were evidenced as a uniform network of red-stained fibrils, which increased in size and density over time (Figure 3a). Quantitative analysis performed after extraction of the dyes showed a statistically significant increase in the amount of collagenous matrix at day 10 as compared with day 5 (Figure 3b). At day 10, the amount of collagenous protein per well (1.9 cm^2) was 5.6 ± 0.1 μg (n = 12). The quantity and quality of the ASC-deposited collagenous matrix in our study appears to be significantly enhanced in comparison to that reported by Guneta et al., in which ASCs were cultured for 28 days before decelullarization with a combined chemical and physical approach [17]. The collagenous matrix content reported in that study was approximately 3 μg per well (from a 96-well plate) and the structural integrity of the scaffold appeared compromised, probably due to the inclusion of three freezing-thawing cycles after the chemical decellularization step.

Immunofluorescence staining allowed revealing the specific molecular identity of the fibrils in the decellularized matrices. While proteomic analysis has shown that ASCs appear to produce a wide range of ECM components [9], we have chosen to investigate the expression of collagens type I and type III, and fibronectin. Collagens type I and III are the major fibrillar constituents of the ECM of the skin, and are thus central to its mechanical properties and are crucial in the remodeling step of the wound healing process. Fibronectin is an ECM glycoprotein, which is also involved in various processes important to wound healing, including cell proliferation, migration and neovascularization [47], and provides the binding sites for several growth factors [48]. Figure 4a are immunofluorescence images that reveal the presence of collagens type I and III, as well as of fibronectin, in the decellularized ECM scaffolds. While type I collagen formed a densely packed array of fibrils, it appeared that type III collagen fibrils

were more loosely arranged. Fibronectin formed a highly branched meshwork of thin fibrils. The fibronectin meshwork appeared to be laid down by the cells on top of the collagen network. This corresponds well with previous studies, which have also shown that matrices produced by ASCs in AA supplemented cultures are rich in collagen I and fibronectin [17]. Overall, it appears that the decellularization method presented here preserves well the microstructural integrity of the deposited ECM. This is in contrast to previous studies using other cellular extraction methods, such as SDS, which significantly compromise the collagen and fibronectin fibrillar networks [20].

As shown in figure 4b, the transcriptional activity of the selected genes during the first three days of induction strongly correlated with the immunofluorescence results described in the previous paragraph. Analysis of the qPCR results showed a time-dependent upregulation on the transcriptional activity of COL1A1 and COL3A1, while expression of MMP1, also known as collagenase-1, was downregulated (Figure 4b). The MMP-1 specifically hydrolyzes type I-III collagens and its over activity has been associated with non-healing wounds [49]. Overall, the gene expression results indicate that there was an enhanced synthesis of collagenous ECM and reduced matrix breakdown. The expression of fibronectin (FN) showed a significant upregulation as well, although only after 72 h.

3.4 Proliferation and morphology of cells cultured on ECM scaffolds

Primary human fibroblasts and endothelial cells (HDMECs) were seeded on different decellularized matrices prepared from cultured ASCs. The rationale for selection of these two cell models was because both cell types play a key role during the cutaneous wound healing process. Fibroblasts not only mediate the effective closure of the wounds but also support the other cells associated with effective healing [50]. Endothelial cell adhesion and proliferation is also crucial in the formation of new blood vessels, which support neovascularization of the granulation tissue that is needed for progression into the healing phase of the wounds [51]. For both cell types, the cytotoxicity/viability assay revealed the presence of a large proportion of viable cells and a negligible number of dead cells, which suggests that the cytotoxic compounds used during decellularization had been washed out (Figure 5a). Phase contrast microscopy after 24 h showed that in both cases the cells were well attached to the ECM substrate (Figure 5b). Moreover, some cells appeared to align over the topographical cues presented by the fibrillar scaffold. Fibroblasts displayed the typical spindle-shaped morphology while HDMECs appeared polygonal, with some thin tube-like protrusions. Interestingly, a study from 2004 by Dye et al. [52] has shown that ECM composition controls the morphological behavior of microvascular endothelial cells, switching their phenotype between migratory and vasculogenic. It remains unknown how signals provided by ASC-derived ECM may influence the morphological behavior and phenotype in these cells, which warrants further studies in this subject. The analysis of cell numbers provided evidence that the scaffolds supported the proliferation of both cell types (Figure 5b). The doubling times calculated from the growth curves were 22.2 ± 5.2 h for the fibroblasts and 27.4 ± 10.6 h for the HDMECs. A thin planar scaffold

(~20 µm) comprising bovine fibrillary collagen I was used as a reference. This collagen cell carrier (CCC) constitutes a suitable substrate for cell culture and allows the transfer of cell sheets obtained from various adherent cell types [53]. Both cell types appeared to grow faster on the ECM than on CCC scaffolds, where fibroblasts and HDMECs displayed a doubling time of 41.7 ± 27.2 h and 59.8 ± 10.5 h, respectively. However, there was no statistically significant difference between the doubling times obtained on ECM vs CCC. The findings from the cell culture assay are in agreement with previous studies, which have shown that scaffolds containing fibronectin and collagen type I provide an optimal support for fibroblasts [54,55] and endothelial cell growth [16,56]. Overall, the decellularized matrices presented here represent a substrate that supports adhesion and proliferation of primary fibroblasts and HDMECs.

While the focus of the present work was on describing a reliable decellularization method as platform for future *in vitro* wound healing studies, it is worth to mention that decellularized cell-derived matrices have also a great potential for application in preclinical research. In this context, a recent *in vivo* study has demonstrated the regenerative potential of ECM scaffolds fabricated by decellularization of BM-MSCs [13].

4. General considerations and hints for troubleshooting

For the induction of cells for ECM production, we recommend the preparation of a sterile stock solution of AA (20 mM, for instance), which must be stored at 4ºC and protected from light. AA should be added to the medium immediately before media changes. It is possible to increase the induction period for more than 10 days to increase the matrix thickness. However, longer incubation times appear to increase the risk of dislodgment of the matrices.

A critical point in the fabrication process remains the proper attachment of the cell-derived ECM to the culture surface. In our experience, although the PLL coating significantly increases the binding of the ECM, the matrices might still detach from the wells if not handled cautiously. It is therefore important to perform all the washes and media changes in a gentle manner during the induction period. Extra caution is also recommended when applying the EB, the DNase solution, and the subsequent washing solutions in order to prevent release of the ECM.

It is also important to perform a uniform cell seeding and monitor the morphology of the ASCs during the induction period. When cells are not uniformly distributed in the wells, they tend to overgrow in certain areas resulting in an inhomogeneous ECM scaffold. We do not recommend using cells that have been cultured for more than five passages, as their proliferation rate and ability to deposit ECM might be severely compromised.

While it appears that 100 UI/mL is the optimal DNase concentration, we recommend determining the optimal enzyme concentration for each new batch of DNase, as the activity of the enzyme might display a significant lot-to-lot variability. It is also important to ensure that the enzyme is dissolved in a buffer containing the divalent Ca^{++} and Mg^{++}. DNAse working solutions should be frozen in aliquots to avoid freeze-thaw cycles. In our experience, an overnight wash after the DNase treatment (>12 h) helps to further dissolve the residual DNA fragments and other cell debris. Shorter washing times might hinder the ability of the scaffolds to support the cell growth.

Using larger culture surfaces to increase the area of the fabricated cell-derived ECM is also possible, as long as the cell seeding density recommended in the methods section is maintained. Transferring of the ECM from the culture plates might be desirable, for example, for implantation studies or to create thicker scaffolds by stacking. In this case, it is possible to perform the culture of ASCs on thermoresponsive culture dishes (Nunc Dishes with UpCell, from ThermoFisher Scientific). After decellularization, the ECM scaffolds are detached from the culture surface by reducing the temperature below 32ºC. Scaffolds can be carefully lifted using the transfer membranes that are supplied with the dishes.

5. Conclusions

The present work is describing a reliable method to obtain extracellular matrices produced by cultured ASCs. The decellularization treatment efficiently removed the cellular components while maintaining a considerable amount of well-preserved extracellular matrix components. The ECM displayed a dense network of fibrillar components (type I and III collagens), as well as a mesh of fibronectin fibrils. Cell growth experiments showed that the decellularized matrices supported growth of fibroblasts and endothelial cells. Overall, ECM scaffolds obtained from ASCs represent a unique biomaterial that has a significant potential for *in vitro* as well as *in vivo* wound healing studies.

Acknowledgments

The authors would like to acknowledge Ole Jensen and Lisa Engen for technical assistance during the laboratory experiments.

Funding

The work was supported in part by funds from the Toyota Foundation and the Obelske Family foundation. The funding sources had no influence on neither study design, collection, analysis, interpretation of data, writing the report, nor decision to submit the paper for publication.

6. Bibliography

[1] S.A. Eming, P. Martin, M. Tomic-Canic, Wound repair and regeneration: mechanisms, signaling, and translation., Sci. Transl. Med. 6 (2014) 265sr6. doi:10.1126/scitranslmed.3009337.

[2] K. Moreo, Understanding and overcoming the challenges of effective case management for patients with chronic wounds, Case Manager. 16 (2005) 62–67. doi:10.1016/j.casemgr.2005.01.014.

[3] T.N. Demidova-Rice, M.R. Hamblin, I.M. Herman, Acute and Impaired Wound Healing, Adv. Skin Wound Care. 25 (2012) 304–314. doi:10.1097/01.ASW.0000416006.55218.d0.

[4] K. Järbrink, G. Ni, H. Sönnergren, A. Schmidtchen, C. Pang, R. Bajpai, J. Car, Prevalence and incidence of chronic wounds and related complications: a protocol for a systematic review, Syst. Rev. 5 (2016). doi:10.1186/s13643-016-0329-y.

[5] V. Zachar, M. Duroux, J. Emmersen, J.G. Rasmussen, C.P. Pennisi, S. Yang, T. Fink, Hypoxia and adipose-derived stem cell-based tissue regeneration and engineering, Expert Opin. Biol. Ther. 11 (2011) 775–786. doi:10.1517/14712598.2011.570258.

[6] J.A. van Dongen, M.C. Harmsen, B. van der Lei, H.P. Stevens, Augmentation of Dermal Wound Healing by Adipose Tissue-Derived Stromal Cells (ASC)., Bioeng. (Basel, Switzerland). 5 (2018). doi:10.3390/bioengineering5040091.

[7] W.U. Hassan, U. Greiser, W. Wang, Role of adipose-derived stem cells in wound healing, Wound Repair Regen. 22 (2014) 313–325. doi:10.1111/wrr.12173.

[8] J.G. Rasmussen, O. Frøbert, L. Pilgaard, J. Kastrup, U. Simonsen, V. Zachar, T. Fink, Prolonged hypoxic culture and trypsinization increase the pro-angiogenic potential of human adipose tissue-derived stem cells, Cytotherapy. 13 (2011) 318–328. doi:10.3109/14653249.2010.506505.

[9] S. Riis, A. Stensballe, J. Emmersen, C.P. Pennisi, S. Birkelund, V. Zachar, T. Fink, Mass spectrometry analysis of adipose-derived stem cells reveals a significant effect of hypoxia on pathways regulating extracellular matrix, Stem Cell Res. Ther. 7 (2016) 52. doi:10.1186/s13287-016-0310-7.

[10] K. Hyldig, S. Riis, C.P. Pennisi, V. Zachar, T. Fink, Implications of extracellular matrix production by adipose tissue-derived stem cells for development of wound healing therapies, Int. J. Mol. Sci. 18 (2017) 1167. doi:10.3390/ijms18061167.

[11] N. Kosaric, H. Kiwanuka, G.C. Gurtner, Stem cell therapies for wound healing, Expert Opin.

Biol. Ther. 19 (2019) 575–585. doi:10.1080/14712598.2019.1596257.

[12] M. Strioga, S. Viswanathan, A. Darinskas, O. Slaby, J. Michalek, Same or Not the Same? Comparison of Adipose Tissue-Derived Versus Bone Marrow-Derived Mesenchymal Stem and Stromal Cells, Stem Cells Dev. 21 (2012) 2724–2752. doi:10.1089/scd.2011.0722.

[13] H.-C. Du, L. Jiang, W.-X. Geng, J. Li, R. Zhang, J.-G. Dang, M.-G. Shu, L.-W. Li, Growth Factor-Reinforced ECM Fabricated from Chemically Hypoxic MSC Sheet with Improved In Vivo Wound Repair Activity, Biomed Res. Int. 2017 (2017) 1–11. doi:10.1155/2017/2578017.

[14] T. Hoshiba, G. Chen, C. Endo, H. Maruyama, M. Wakui, E. Nemoto, N. Kawazoe, M. Tanaka, Decellularized extracellular matrix as an in vitro model to study the comprehensive roles of the ECM in stem cell differentiation, Stem Cells Int. 2016 (2016). doi:10.1155/2016/6397820.

[15] R. Rakian, T.J. Block, S.M. Johnson, M. Marinkovic, J. Wu, Q. Dai, D.D. Dean, X.-D. Chen, Native extracellular matrix preserves mesenchymal stem cell "stemness" and differentiation potential under serum-free culture conditions, Stem Cell Res. Ther. 6 (2015) 235. doi:10.1186/s13287-015-0235-6.

[16] Y. Xu, M. Yan, Y. Gong, L. Chen, F. Zhao, Z. Zhang, Response of endothelial cells to decellularized extracellular matrix deposited by bone marrow mesenchymal stem cells., Int. J. Clin. Exp. Med. 7 (2014) 4997–5003. http://www.ncbi.nlm.nih.gov/pubmed/25663998 (accessed March 1, 2019).

[17] V. Guneta, Z. Zhou, N.S. Tan, S. Sugii, M.T.C. Wong, C. Choong, Recellularization of decellularized adipose tissue-derived stem cells: role of the cell-secreted extracellular matrix in cellular differentiation, Biomater. Sci. 6 (2018) 168–178. doi:10.1039/C7BM00695K.

[18] H. Lu, T. Hoshiba, N. Kawazoe, I. Koda, M. Song, G. Chen, Cultured cell-derived extracellular matrix scaffolds for tissue engineering., Biomaterials. 32 (2011) 9658–66. doi:10.1016/j.biomaterials.2011.08.091.

[19] H. Lu, T. Hoshiba, N. Kawazoe, G. Chen, Comparison of decellularization techniques for preparation of extracellular matrix scaffolds derived from three-dimensional cell culture, J. Biomed. Mater. Res. Part A. 100A (2012) n/a-n/a. doi:10.1002/jbm.a.34150.

[20] Q. Xing, K. Yates, M. Tahtinen, E. Shearier, Z. Qian, F. Zhao, Decellularization of Fibroblast Cell Sheets for Natural Extracellular Matrix Scaffold Preparation, Tissue Eng. Part C Methods. 21 (2015) 77–87. doi:10.1089/ten.tec.2013.0666.

[21] L.E. Fitzpatrick, T.C. McDevitt, Cell-derived matrices for tissue engineering and regenerative medicine applications., Biomater. Sci. 3 (2015) 12–24. doi:10.1039/C4BM00246F.

[22] G.M. Harris, I. Raitman, J.E. Schwarzbauer, Cell-derived decellularized extracellular matrices, in: Methods Cell Biol., Academic Press, 2018: pp. 97–114. doi:10.1016/bs.mcb.2017.08.007.

[23] J. Franco-Barraza, D.A. Beacham, M.D. Amatangelo, E. Cukierman, Preparation of extracellular matrices produced by cultured and primary fibroblasts, Curr. Protoc. Cell Biol. 2016 (2016) 10.9.1-10.9.34. doi:10.1002/cpcb.2.

[24] M. Marinkovic, T.J. Block, R. Rakian, Q. Li, E. Wang, M.A. Reilly, D.D. Dean, X.-D. Chen, One size does not fit all: developing a cell-specific niche for in vitro study of cell behavior, Matrix Biol. 52–54 (2016) 426–441. doi:10.1016/J.MATBIO.2016.01.004.

[25] R.P. Gersch, J.C. Raum, C. Calvert, I. Percec, Fibroblasts Derived From Human Adipose Stem Cells Produce More Effective Extracellular Matrix and Migrate Faster Compared to Primary Dermal Fibroblasts, Aesthetic Surg. J. (2019). doi:10.1093/asj/sjz071.

[26] V. Zachar, J.G. Rasmussen, T. Fink, Isolation and growth of adipose tissue-derived stem cells., in: Methods Mol. Biol., Humana Press, 2011: pp. 37–49. doi:10.1007/978-1-60761-999-4_4.

[27] F.M. Nielsen, S.E. Riis, J.I. Andersen, R. Lesage, T. Fink, C.P. Pennisi, V. Zachar, Discrete adipose-derived stem cell subpopulations may display differential functionality after in vitro expansion despite convergence to a common phenotype distribution, Stem Cell Res. Ther. 7 (2016) 211. http://stemcellres.biomedcentral.com/articles/10.1186/s13287-016-0435-8.

[28] S. Riis, F.M. Nielsen, C.P. Pennisi, V. Zachar, T. Fink, Comparative Analysis of Media and Supplements on Initiation and Expansion of Adipose-Derived Stem Cells, Stem Cells Transl. Med. 5 (2016) 314–324. doi:10.5966/sctm.2015-0148.

[29] S. Riis, R. Newman, H. Ipek, J.I. Andersen, D. Kuninger, S. Boucher, M.C. Vemuri, C.P. Pennisi, V. Zachar, T. Fink, Hypoxia enhances the wound-healing potential of adipose-derived stem cells in a novel human primarykeratinocyte-based scratch assay, Int. J. Mol. Med. 39 (2017). doi:10.3892/ijmm.2017.2886.

[30] S. Riis, A. Stensballe, J. Emmersen, C.P. Pennisi, S. Birkelund, V. Zachar, T. Fink, Mass spectrometry analysis of adipose-derived stem cells reveals a significant effect of hypoxia on pathways regulating extracellular matrix, Stem Cell Res. Ther. 7 (2016) 52. doi:10.1186/s13287-016-0310-7.

[31] S. Foldberg, M. Petersen, P. Fojan, L. Gurevich, T. Fink, C.P. Pennisi, V. Zachar, Patterned poly(lactic acid) films support growth and spontaneous multilineage gene expression of adipose-derived stem cells, Colloids Surfaces B Biointerfaces. (2012). doi:10.1016/j.colsurfb.2011.12.018.

[32] L. Pilgaard, P. Lund, M. Duroux, T. Fink, M. Ulrich-Vinther, K. Søoballe, V. Zachar, Effect of oxygen concentration, culture format and donor variability on in vitro chondrogenesis of human adipose tissue-derived stem cells, Regen. Med. 4 (2009) 539–548.

[33] P. Lund, L. Pilgaard, M. Duroux, T. Fink, V. Zachar, Effect of growth media and serum replacements on the proliferation and differentiation of adipose-derived stem cells, Cytotherapy. 11 (2009) 189–197. http://informahealthcare.com/doi/abs/10.1080/14653240902736266.

[34] T. Fink, P. Lund, L. Pilgaard, J.G. Rasmussen, M. Duroux, V. Zachar, Instability of standard PCR reference genes in adipose-derived stem cells during propagation, differentiation and hypoxic exposure., BMC Mol. Biol. 9 (2008) 98. doi:10.1186/1471-2199-9-98.

[35] C.P. Pennisi, V. Zachar, T. Fink, L. Gurevich, P. Fojan, Patterned polymeric surfaces to study the influence of nanotopography on the growth and differentiation of mesenchymal stem cells, 2013. doi:10.1007/7651-2013-10.

[36] K.-M. Choi, Y.-K. Seo, H.-H. Yoon, K.-Y. Song, S.-Y. Kwon, H.-S. Lee, J.-K. Park, Effect of ascorbic acid on bone marrow-derived mesenchymal stem cell proliferation and differentiation, J. Biosci. Bioeng. 105 (2008) 586–594. doi:10.1263/jbb.105.586.

[37] R.-I. Hata, H. Senoo, L-ascorbic acid 2-phosphate stimulates collagen accumulation, cell proliferation, and formation of a three-dimensional tissuelike substance by skin fibroblasts, J. Cell. Physiol. 138 (1989) 8–16. doi:10.1002/jcp.1041380103.

[38] M. Vermette, V. Trottier, V. Ménard, L. Saint-Pierre, A. Roy, J. Fradette, V. Trottiera, V. Ménarda, L. Saint-Pierrea, A. Roy, J. Fradette, Production of a new tissue-engineered adipose substitute from human adipose-derived stromal cells, Biomaterials. 28 (2007) 2850–2860. doi:10.1016/j.biomaterials.2007.02.030.

[39] C. D'Aniello, F. Cermola, E.J. Patriarca, G. Minchiotti, Vitamin C in Stem Cell Biology: Impact on Extracellular Matrix Homeostasis and Epigenetics, Stem Cells Int. 2017 (2017). doi:10.1155/2017/8936156.

[40] K. Fujisawa, K. Hara, T. Takami, S. Okada, T. Matsumoto, N. Yamamoto, I. Sakaida, Evaluation of the effects of ascorbic acid on metabolism of human mesenchymal stem cells, Stem Cell Res. Ther. 9 (2018) 93. doi:10.1186/s13287-018-0825-1.

[41] T. Hoshiba, C.S. Cho, A. Murakawa, Y. Okahata, T. Akaike, The effect of natural extracellular matrix deposited on synthetic polymers on cultured primary hepatocytes, Biomaterials. 27 (2006) 4519–4528. doi:10.1016/J.BIOMATERIALS.2006.04.014.

[42] H. Kim, Y. Kim, M. Fendereski, N.S. Hwang, Y. Hwang, Recent Advancements in Decellularized Matrix-Based Biomaterials for Musculoskeletal Tissue Regeneration, in: Adv. Exp. Med. Biol., Springer, Singapore, 2018: pp. 149–162. doi:10.1007/978-981-13-0947-2_9.

[43] P.M. Crapo, T.W. Gilbert, S.F. Badylak, An overview of tissue and whole organ decellularization processes, Biomaterials. 32 (2011) 3233–3243. doi:10.1016/j.biomaterials.2011.01.057.

[44] A.Y. Alekseeva, N. V. Bulycheva, S. V. Kostyuk, T.D. Smirnova, N.N. Veiko, Cell Free DNA (cfDNA) Influences Nitric Oxide and ros Levels in Human Endothelial Cells, in: Circ. Nucleic Acids Plasma Serum, Springer Netherlands, Dordrecht, 2010: pp. 219–223. doi:10.1007/978-90-481-9382-0_30.

[45] S. Nagata, R. Hanayama, K. Kawane, Autoimmunity and the Clearance of Dead Cells, Cell. 140 (2010) 619–630. doi:10.1016/j.cell.2010.02.014.

[46] Y.K. Noh, P. Du, I.G. Kim, J. Ko, S.W. Kim, K. Park, Polymer mesh scaffold combined with cell-derived ECM for osteogenesis of human mesenchymal stem cells, Biomater. Res. 20 (2016) 6. doi:10.1186/s40824-016-0055-5.

[47] R.A.F. Clark, Fibronectin Matrix Deposition and Fibronectin Receptor Expression in Healing and Normal Skin, J. Invest. Dermatol. 94 (1990) s128–s134. doi:10.1111/1523-1747.EP12876104.

[48] J. Zhu, R.A.F. Clark, Fibronectin at Select Sites Binds Multiple Growth Factors and Enhances their Activity: Expansion of the Collaborative ECM-GF Paradigm, J. Invest. Dermatol. 134 (2014) 895–901. doi:10.1038/JID.2013.484.

[49] M.P. Caley, V.L.C. Martins, E.A. O'Toole, Metalloproteinases and Wound Healing, Adv. Wound Care. 4 (2015) 225–234. doi:10.1089/wound.2014.0581.

[50] B. P., Wound healing and the role of fibroblasts, J. Wound Care. 22 (2013) 407–412. doi:10.12968/jowc.2013.22.8.407.

[51] S.M. Bauer, R.J. Bauer, O.C. Velazquez, Angiogenesis, Vasculogenesis, and Induction of Healing in Chronic Wounds, Vasc. Endovascular Surg. 39 (2005) 293–306. doi:10.1177/153857440503900401.

[52] J.F. Dye, L. Lawrence, C. Linge, L. Leach, J.A. Firth, P. Clark, Distinct Patterns of Microvascular Endothelial Cell Morphology Are Determined by Extracellular Matrix Composition, Endothelium. 11 (2004) 151–167. doi:10.1080/10623320490512093.

[53] T. Schmidt, S. Stachon, A. Mack, M. Rohde, L. Just, Evaluation of a Thin and Mechanically

Stable Collagen Cell Carrier, Tissue Eng. Part C Methods. 17 (2011) 1161–1170. http://www.liebertonline.com/doi/abs/10.1089/ten.tec.2011.0201.

[54] M. Cimini, D.R. Boughner, J.A. Ronald, D.E. Johnston, K.A. Rogers, Dermal fibroblasts cultured on small intestinal submucosa: Conditions for the formation of a neotissue, J. Biomed. Mater. Res. Part A. 75A (2005) 895–906. doi:10.1002/jbm.a.30493.

[55] J. Sapudom, X. Wu, M. Chkolnikov, M. Ansorge, U. Anderegg, T. Pompe, Fibroblast fate regulation by time dependent TGF-β1 and IL-10 stimulation in biomimetic 3D matrices., Biomater. Sci. 5 (2017) 1858–1867. doi:10.1039/c7bm00286f.

[56] M. Sgarioto, P. Vigneron, J. Patterson, F. Malherbe, M.-D. Nagel, C. Egles, Collagen type I together with fibronectin provide a better support for endothelialization, C. R. Biol. 335 (2012) 520–528. doi:10.1016/j.crvi.2012.07.003.

Figure legends

Figure 1. Assessment of culture conditions to produce homogeneous and stable cell sheets. The diagrams indicate the different conditions. AA: induction with ascorbic acid. PLL: poly-L-Lysine coating prior to cell seeding. Control are untreated wells without AA supplementation. Phase contrast images display cells after 10 days in culture. The black arrow indicates the edge of a cell sheet that is detaching from the well surface in the right to left direction. Scale bars depict 200 µm.

Figure 2. Confirmation of decellularization and assessment of the optimal DNAse concentration. (a) Fluorescence microscopy images displaying the residual DNA fragments after treatment of the ASCs sheets with the EB (control) and upon incubation with different DNase concentrations. DNA fragments were stained with Hoechst 33342 nuclear stain (blue) (b) Phase contrast microscopy images displaying the morphology of the ECM scaffolds before and after treatment with 100 U/mL of DNase. (c) Quantification of the amount of dsDNA by the PicoGreen assay, showing a reduction of DNA content upon treatment with the DNase solutions. Asterisks indicate statistically significant difference as compared to the control or between the treatment groups ($n = 9$, ** $p<0.001$, * $p<0.01$). Scale bars depict 200 µm.

Figure 3. Analysis of ECM production by cells over time. (a) Brightfield microscopy images after Sirius Red/Fast Green staining, showing the quality of collagenous matrix deposited by the ASCs after 5 and 10 days of induction. (b) Quantification of the amount of collagen deposited by the ASCs. Asterisk indicates statistically significant difference ($n=12$, $p<0.001$). Scale bar depict 200 µm.

Figure 4. Assessment of composition of the cell-deposited ECM. (a) Fluorescence microscopy images displaying the structure and specific molecular composition of the ECM after immunostaining with antibodies against collagen type I, type III, or fibronectin. (b) Results of the semi-quantitative PCR assay, reflecting the levels of transcriptional activity of COL1A1 (Col I), COL3A1 (Col III), MMP1, and FN genes in ASCs during the three first days of the induction period. The expression levels were normalized to the control gene PPIA. Asterisks indicate statistically significant difference as compared to the expression level at 24 h ($n=3$, $p<0.05$). Scale bars depict 200 µm.

Figure 5. Growth of cells on the ASCs derived matrices. Panels (a) and (b) show the cells after 24 h of culture on the ECM scaffolds. (a) Fluorescence images of the cells after the live/dead staining, displaying the live cells in green and the dead cells in red. Scale bars depict 300 µm. (b) Phase contrast

microscopy images displaying the adhesion patterns and the morphology of cells. Scale bars depict 200 µm. Panels (c) and (d) are the growth curves obtained after regression analysis, showing a sustained proliferation of both cell types on the ECM scaffolds and on the collagen cell carriers (CCC). The growth curves corresponding to fibroblasts and HDMECs are shown in (c) and (d), respectively.

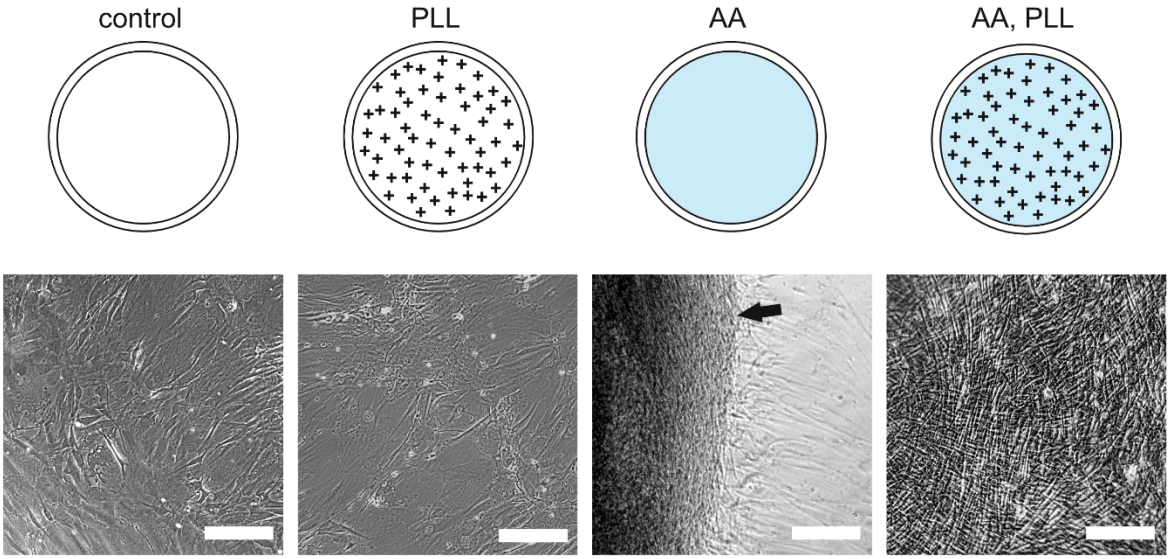

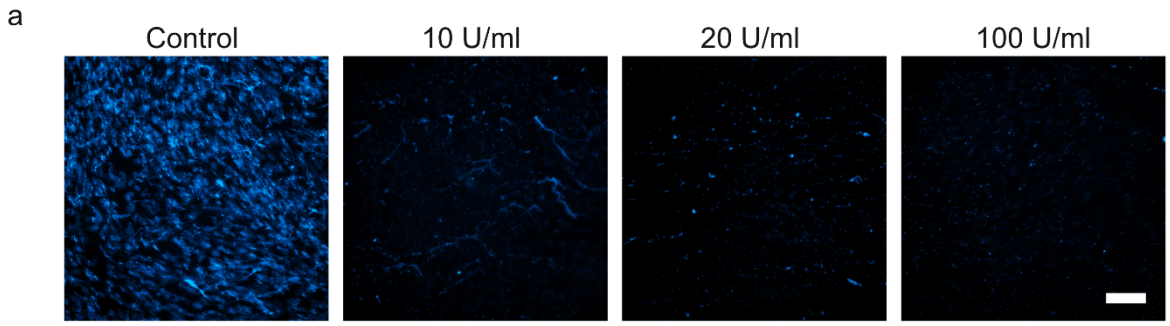

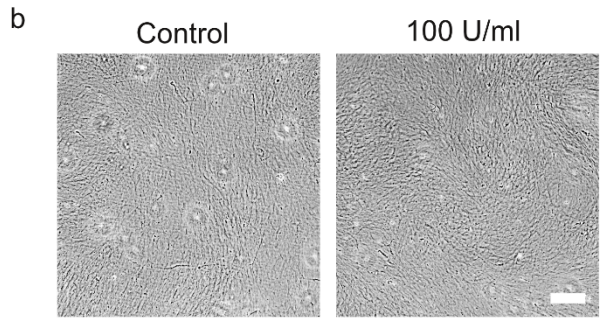

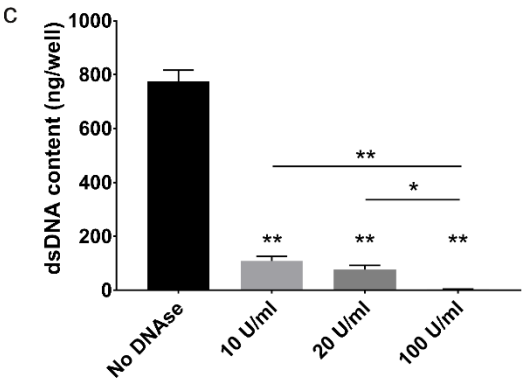

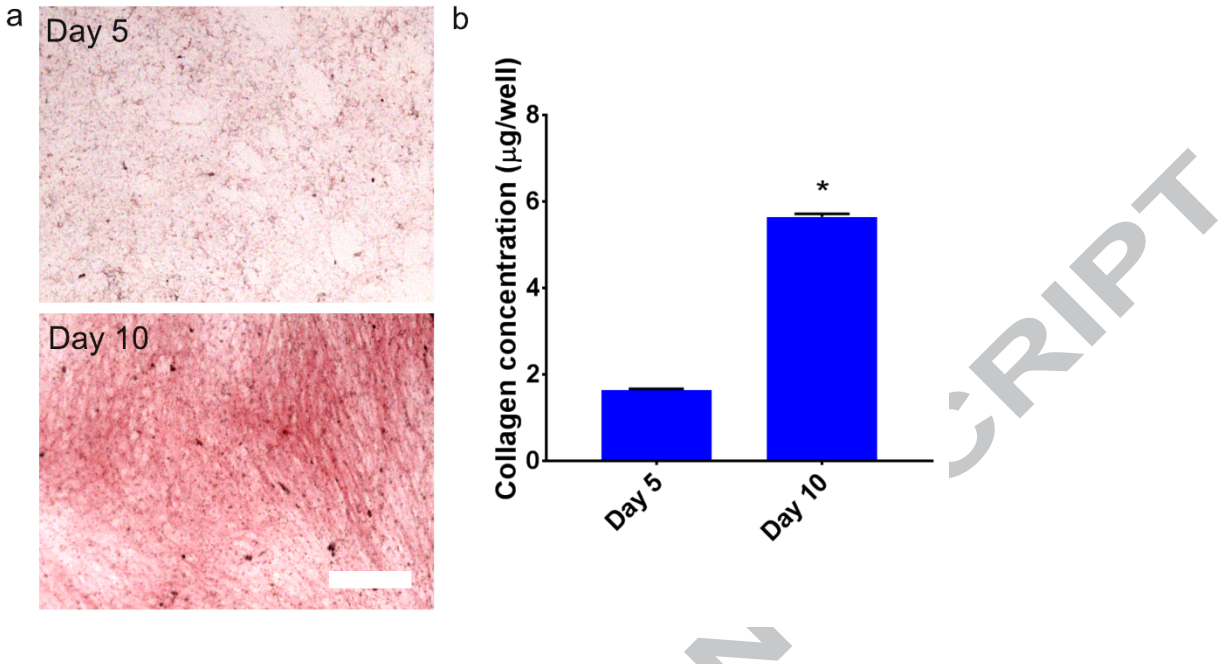

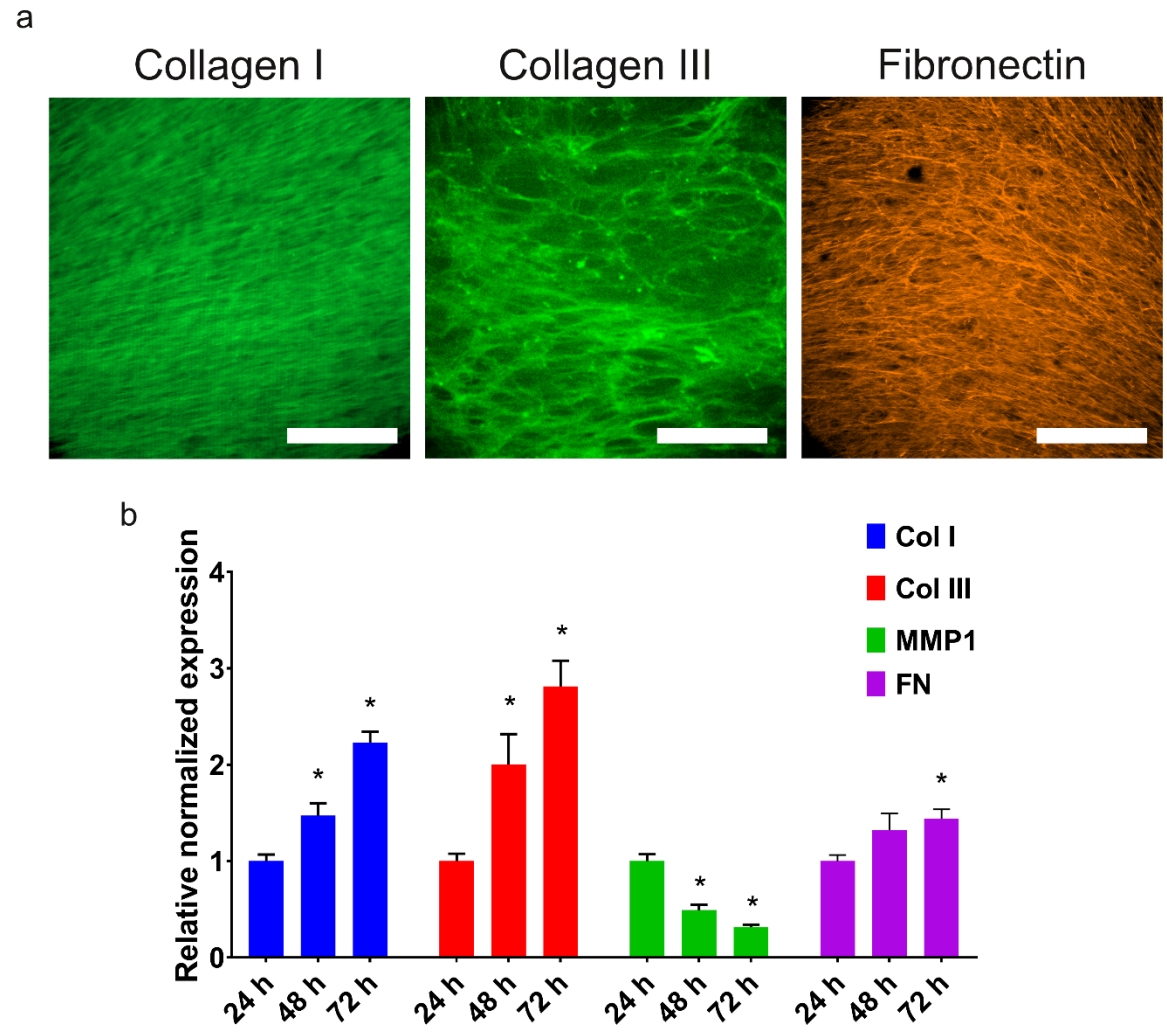

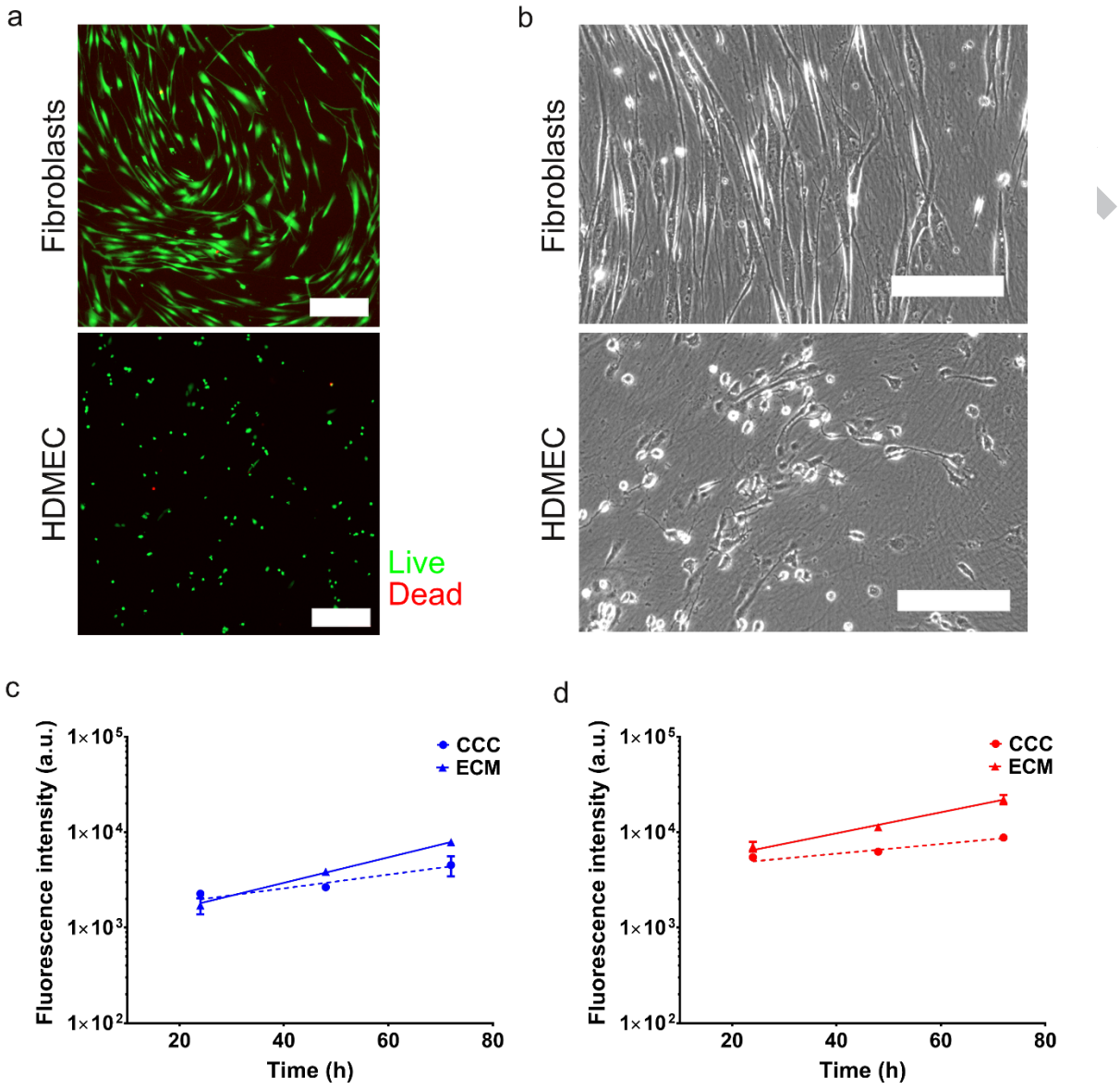

Table I: List of genes, primer sequences, and annealing temperatures (AT) used in this study.

Gene symbol	Gene description	Primer base sequence (5'-3')		AT (°C)
		Forward	Reverse	
COL1A1	Collagen type I alpha 1	CCT GGA TGC CAT CAA AGT CT	AAT CCA TCG GTC ATG CTC TC	62
COL3A1	Collagen type III alpha 1	TAC GGC AAT CCT GAA CTT CC	GTG TGT TTC GTG CAA CCA TC	61

MMP-1	Matrix metalloproteinase 1	TGT GGT GTC TCA CAG CTT CC	CAC TGG GCC ACT ATT TCT CC	62
Fn	Fibronectin	ACC TAC GGA TGA CTC GTG CTT TGA	CAA AGC CTA AGC ACT GGC ACA ACA	62
PPIA	Peptidylprolyl isomerase A	TCC TGG CAT CTT GTC CAT G	CCA TCC AAC CAC TCA GTC TTG	60

- Extracellular matrix (ECM) scaffolds are fabricated from cultured adipose-derived stem cells (ASCs)

- Methods to assess the molecular composition and biological properties of the ECM are presented

- The microstructure and native constituents are preserved in the scaffolds

- The decellularized scaffolds provide a useful platform to study the role of ECM deposited by ASCs in wound healing